Altermagnetic Shastry-Sutherland fullerene networks

Jiaqi Wu,^{1,*} Alaric Sanders,^{2,*} Rundong Yuan,² and Bo Peng^{2,†}

¹Peterhouse, University of Cambridge, Trumpington Street, Cambridge CB2 1RD, UK

²Theory of Condensed Matter Group, Cavendish Laboratory, University

of Cambridge, J. J. Thomson Avenue, Cambridge CB3 0HE, UK

(Dated: August 29, 2025)

Abstract

Molecular building blocks provide a versatile platform for realising exotic quantum phases. Using charge neutral, pure carbon fullerene molecules as an example, we design altermagnetic C_{40} monolayers in Shastry-Sutherland lattice. The resonance structure of one unpaired electron leads to an effective spin-1/2 cluster on both long sides of the molecule, which, after rotating into a 2D rutile-like crystal structure, forms altermagnetic ground state. We show d-wave spitting of the spin-polarised electronic band structure and strong chiral-split magnon bands. Most interestingly, the effective spin-1/2 clusters form the Shastry-Sutherland model with a rich phase diagram including altermagenti, quantum spin liquid, plaquette, and dimer phases, which can be easily accessed to via moderate bi-axial strains. Our findings present magnetic fullerene monolayers as a tunable platform for exotic quantum magnetism and spintronic applications.

^{*} equal author contribution

[†] bp432@cam.ac.uk

INTRODUCTION

Altermagnets have attracted great interest as prospective materials for next-generation spintronics. Altermagnetic systems have zero net magnetisation similar to antiferromagnets due to the full cancellation of magnetic moments enforced by lattice symmetry. However, due to the lack of inversion of translational symmetry between spin-up and spin-down sublattices, the band structure shows finite spin-splitting along certain directions in the Brillouin zone. Theoretical investigations have explored the interplay of geometric frustration and altermagnetic order in well-known toy models such as the Shastry-Sutherland lattice. However, most known altermagnets are inorganic atomic crystals, such as RuO₂, MnTe and CrSb, which limits the experimental feasibility and structural tuneability for realising exotic spin models such as the Shastry-Sutherland lattice.

Molecular building blocks are promising alternatives to atomic lattices due to their stable units and highly tuneable structures. Since the synthesis of polymeric C_{60} monolayers, fullerene monolayers have attracted great attention in applications such as heterogeneous catalysis. Recently, we have proposed a way to systematically introduce magnetism in fullerene monolayers through lattice symmetry and further demonstrated the potential of magnetic fullerene monolayers as tuneable topological materials. Here, we design altermagnetic Shastry-Sutherland lattice based on polymeric C_{40} . Counterintuitively, the unpaired electrons in resonance structures of these fullerene monolayers exhibit effective spin-1/2 behaviours and can be continuously tuned into the frustrated quantum spin liquid phase through moderate strain.

METHODS

Density functional theory (DFT) calculations are performed using the Vienna *ab initio* Simulation Package (VASP) under the general gradient approximation (GGA) formalism with plane-augmented wave (PAW) basis sets. The Perdew-Burke-Ernzerhof functional corrected for solids (PBEsol) is used along with C $2s^22p^2$ as valence electrons. A plane-wave cutoff of 800 eV is employed and the self-consistent field energy convergence criterion is set to 10^{-6} eV. The Brillouin zone is sampled with a converged **k**-mesh of 3×3 (see Supplementary Material for convergence tests). The crystal structures are fully relaxed until the Hellmann-

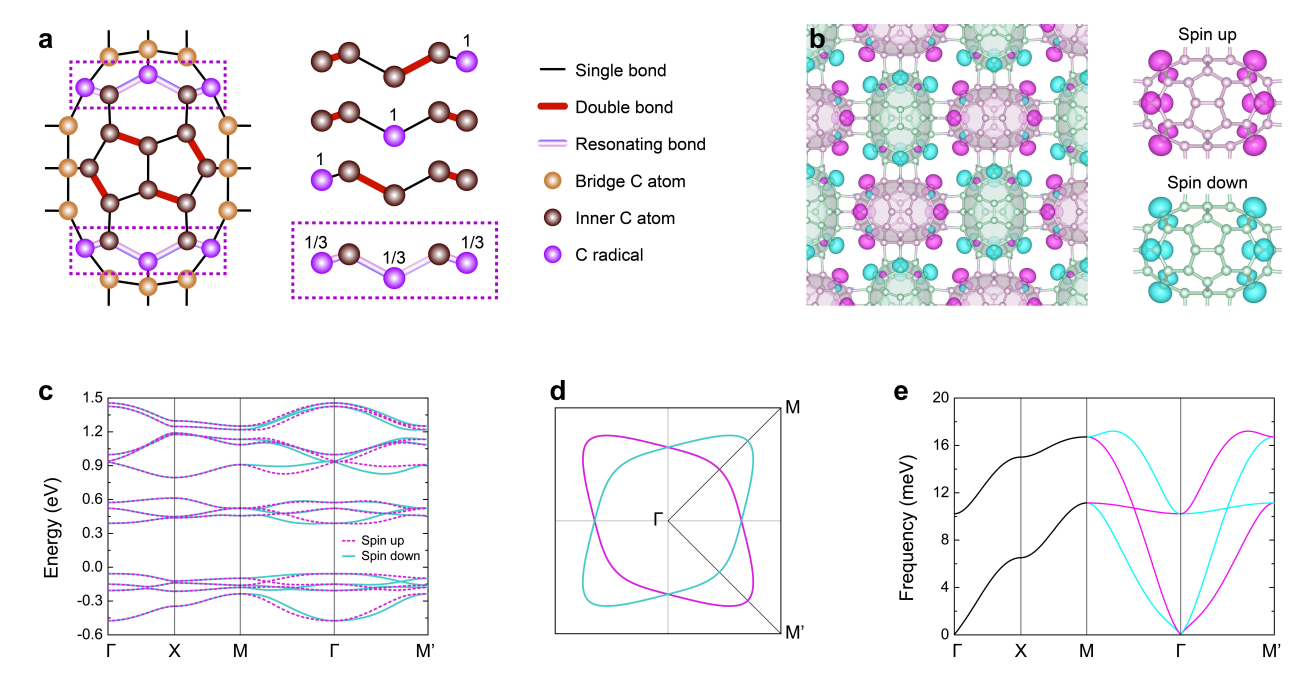


FIG. 1. Altermagnetism in monolayer C_{40} fullerene networks. a C_{40} building block and its resonance structures, **b** spin densities, **c** band structures, **d** iso-energy surface at $0.025 \,\text{eV}$ below the VBM for d-wave order, and **e** chiral-split magnons.

Feynman forces are less than $10^{-2} \,\mathrm{eV\AA}^{-1}$. The vacuum spacing between monolayers were set to more than 20 Å, and dipole corrections are employed perpendicular to the monolayers to eliminate interactions between periodic images. A Wannier function tight-binding model is constructed using Wannier90 by projecting Wannier functions onto each σ bond centre, with sp^2 carbon atoms having an extra Wannier function to mimic the p_z orbitals. The exchange interactions are computed using the TB2J package. To analyse the effect of strain, the lattice parameters are modified (with respect to the fully relaxed structure) and fixed, while the atomic coordinates are allowed to relax.

RESULTS

Crystal structures and magnetic properties

Figure 1a shows the basic building blocks of altermagnetic Shastry-Sutherland fullerene networks. There are 12 fully-saturated carbon atoms with sp^3 hybridization for intermolecular bonds (marked in yellow). For the 8 carbon atoms forming the two five-membered rings in the centre of C_{40} , each atom is surrounded by three single bonds due to the sp^2 hybridi-

sation, leaving one p_z electron to form double bond as marked by red in Fig. 1a. For the five carbon atoms in the W shape (as highlighted in the purple box), there are three pairing schemes for the two double bonds, leaving one unpaired electron at the leftmost, middle and rightmost sites, respectively. The resonance structure leads to an averaged distribution of $1/3 \mu_{\rm B}$ magnetic moment per purple carbon atom and a quantised total magnetic moment of $1 \mu_{\rm B}$ for the group of five atoms in the W-shaped chain.

Rotating neighbouring C_{40} building blocks by $\pi/2$ creates a 2D rutile-like lattice similar to RuO_2 , leading to the altermagnetic ground state (as discussed later). Figure 1b shows the corresponding spin densities where magenta (cyan) iso-surface represents spin-up (spin-down) states. The distribution of spins confirms the resonance structure for 1/3 μ_B per magnetic carbon atom.

We next examine the band structures of altermagnetic C_{40} networks in Fig. 1c. The spinup and spin-down states are doubly degenerate along the Γ -X-M high-symmetry paths and become split along M- Γ -M'. We further compute the iso-energy surface at 0.025 eV below the valence band maximum (VBM), which corresponds to moderate hole doping. As shown in Fig. 1d, the iso-energy surface exhibits typical features for d-wave order, which is similar to RuO₂.

To further confirm the altermagnetic order, we compute the magnon dispersion based on the bosonic Hamiltonian [1] under the Holstein-Primakoff transformation [2], as implemented in the MAGNOPY package that has been widely employed to study low-dimensional antiferromagnets [3, 4]. As shown in Fig. 1e, the low-frequency magnon dispersion near Γ shows linear dispersion, showing typical antiferromagnetic/altermagnetic features. The degenerate magnon bands along Γ -X-M exhibit giant chiral splitting along M- Γ -M'. All magnon frequencies are non-negative with a global minimum at Γ , confirming the altermagnetic ground state [5].

Exchange interactions

We then examine the exchange interactions in altermagnetic C_{40} monolayers. As shown in Fig. 2a, the exchange interactions between atoms within one effective spin-1/2 group are denoted as J_{ii} , the intramolecular interactions between the two effective spin-1/2 groups are denoted as $J_{ii'}$, while the intermolecular interactions from the nearest neighbouring effective

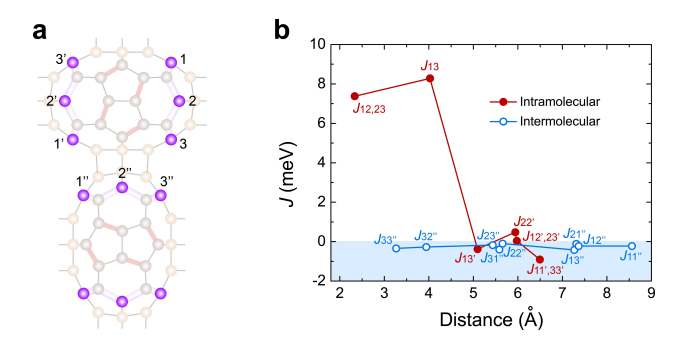


FIG. 2. Exchange interactions in altermagnetic C_{40} monolayers. a Magnetic carbon atoms and **b** their corresponding exchange interactions as a function of distance.

spin-1/2 group are denoted as $J_{ii''}$.

Figure 2b summarises the calculated J parameters as a function of distance between these magnetic atoms. Within one effective spin-1/2 group, the ferromagnetic interactions are dominant ($J_{ii} > 7 \,\text{meV}$). Intramolecular $J_{ii'}$ coupling is much smaller (between -0.9 and $0.5 \,\text{meV}$), and the antiferromagnetic couplings ($J_{13'} = -0.38 \,\text{meV}$, $J_{11'} = J_{33'} = -0.90 \,\text{meV}$) are stronger the ferromagnetic ones ($J_{22'} = 0.48 \,\text{meV}$, $J_{12'} = J_{23'} = 0.04 \,\text{meV}$). The intermolecular interactions are all antiferromagnetic, with much weaker interaction strength than that of the intramolecular coupling. The largest intermolecular coupling comes from atom 1 and atom 3" ($J_{13''} = -0.42 \,\text{meV}$), whereas the smallest intermolecular coupling corresponds to $J_{22''} = -0.10 \,\text{meV}$. The intermolecular interactions beyond the nearest neighbouring group quickly decay to zero.

Phase diagram

Having understood the exchange interactions of monolayer C_{40} networks, we can build a lattice spin model by treating the three magnetic atoms in the effective spin-1/2 group as one spin-1/2 site. This leads to the well-known Shastry-Sutherland model, as shown in Fig. 3a. The exchange interactions between these effective spin-1/2 sites can be divided into two groups – intramolecular exchange J_0 (marked in dark red) and intermolecular exchange J_1 (marked in blue). The effective exchange interactions can be defined as

$$J_{\text{eff}} = \frac{\sum S_i^{(1)} J_{ij} S_j^{(2)}}{\sum S_i^{(1)} \sum S_j^{(2)}},\tag{1}$$

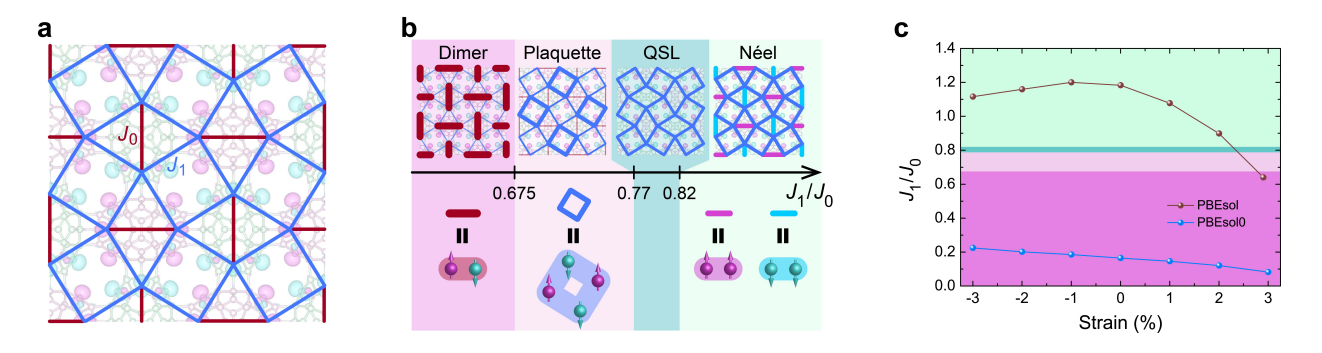


FIG. 3. Phase diagram of Shastry-Sutherland C_{40} fullerene networks. a Shastry-Sutherland lattice, **b** phase diagram, and **c** order parameter J_1/J_0 as a function of bi-axial strain computed from semi-local PBEsol and hybrid-functional PBEsol0.

where $S_i^{(1)}$ and $S_j^{(2)}$ indicate electron spin from atomic site *i* from effective spin-1/2 cluster 1 and atomic site *j* from effective cluster 2 respectively.

The phase diagram can be tuned by the ratio between intermolecular and intramolecular coupling J_1/J_0 . When the intramolecular J_0 dominates, the two spins on each fullerene pair up into a singlet state. This is known as the dimer valence bond solid phase, where neighbouring singlet pairs do not talk to each other. Slightly increasing the J_1/J_0 ratio above 0.675 results in a similar phase of independent "plaquette" units consisting of four spins. In the fullerene lattice this corresponds to four spins located on four molecules around an interstice. When J_1/J_0 lies between 0.77 and 0.82, a quantum spin liquid phase is formed due to the frustrations between the intramolecular and intermolecular exchange couplings. Such exotic phases have promising applications such as error-resistant qubits due to long-range correlations. In the other extreme where J_1 dominates over J_0 , the Shastry-Sutherland lattice effectively reduces to the altermagnetic phase with a Néel ground state. Each fullerene molecule is located at a corner of a square. The two spins within one single fullerene are the same, whereas neighbouring fullerene molecules have opposite spins, which is exactly the ground-state altermagnetic phase we find in *ab initio* calculations.

To tune the ratios between J_1 and J_0 , we introduce bi-axial strains. Figure 3 c shows the J_1/J_0 ratios computed for monolayer C_{40} networks under varied strain. At the DFT level of theory, the ground state under zero strain is the Néel order, consistent with previous magnon data. As the strain is increased to 2-3%, the C_{40} system passes through both the quantum spin liquid and plaquette phases, until reaching the dimer region. Further hybrid functional calculations suggest that the dimer phase is stable at all strains between $\pm 3\%$, suggesting

the tuneability for various phases through control of screening effects via substracts. The realisation of the Shastry-Sutherland lattice in monolayer C_{40} networks provides oppurtunities for observing exotic physics in molecular materials compared to previous atomic systems.

CONCLUSION

Using monolayer C_{40} networks as an example, we demonstrate the feasibility of realising exotic spin phases based on molecular building blocks, as manifested in our single-element, charge-neutral carbon systems. Here we demonstrate the altermagnetic phase as a proof-of-principle study, which, counterintuitively, exhibits strong chiral splitting in magnons. We also stress that these systems have much richer physics beyond altermagnetic order such as the emergence of quantum spin liquid phase. Our work opens a new avenue in realising exotic spin physics in pure carbon-based systems.

- [1] J.H.P. Colpa, "Diagonalization of the quadratic boson hamiltonian," Physica A: Statistical Mechanics and its Applications 93, 327–353 (1978).
- [2] T. Holstein and H. Primakoff, "Field dependence of the intrinsic domain magnetization of a ferromagnet," Phys. Rev. **58**, 1098–1113 (1940).
- [3] Andrey Rybakov, Carla Boix-Constant, Diego Alba Venero, Herre S. J. van der Zant, Samuel Mañas-Valero, and Eugenio Coronado, "Probing short-range correlations in the van der waals magnet crsbr by small-angle neutron scattering," Small Sci. 4, 2400244– (2024).
- [4] Carla Boix-Constant, Andrey Rybakov, Clara Miranda-Pérez, Gabriel Martínez-Carracedo, Jaime Ferrer, Samuel Mañas-Valero, and Eugenio Coronado, "Programmable magnetic hysteresis in orthogonally-twisted 2d crsbr magnets via stacking engineering." Adv. Mater. 37, 2415774— (2025).
- [5] Andres Tellez-Mora, Xu He, Eric Bousquet, Ludger Wirtz, and Aldo H. Romero, "Systematic determination of a material's magnetic ground state from first principles," npj Computational Materials 10, 20 (2024).